

1 **ChAdOx1 nCoV-19 (AZD1222) vaccine elicits monoclonal antibodies with potent cross-**
2 **neutralizing activity against SARS-CoV-2 viral variants**

3

4 Jeffrey Seow,^{1*} Carl Graham,^{1*} Sadie R. Hallett,¹ Thomas Lechmere,¹ Thomas J.A. Maguire,¹
5 Isabella Huettner,¹ Daniel Cox,¹ Rebekah Roberts,² Anele Waters,² Christopher C. Ward,¹
6 Christine Mant,³ Michael J. Pitcher,⁴ Jo Spencer,⁴ Julie Fox,^{1,2} Michael H. Malim,¹ Katie J.
7 Doores^{1#}

8

9 ¹ Department of Infectious Diseases, School of Immunology & Microbial Sciences, King's
10 College London, London, UK.

11 ² Harrison Wing, Guys and St Thomas' NHS Trust, London, UK.

12 ³ Infectious Diseases Biobank, Department of Infectious Diseases, School of Immunology
13 and Microbial Sciences, King's College London, London, UK.

14 ⁴ Peter Gorer Department of Immunobiology, School of Immunology & Microbial Sciences,
15 King's College London, London, UK.

16

17

18 * These authors contributed equally

19 # Corresponding author: katie.doores@kcl.ac.uk

20

21 **Abstract**

22 Although the antibody response to COVID-19 vaccination has been studied extensively at the
23 polyclonal level using immune sera, little has been reported on the antibody response at the
24 monoclonal level. Here we isolate a panel of 44 anti-SARS-CoV-2 monoclonal antibodies
25 (mAbs) from an individual who received two doses of the ChAdOx1 nCoV-19 (AZD1222)
26 vaccine at a 12-week interval. We show that despite a relatively low serum neutralization titre,
27 mAbs with potent neutralizing activity against the current SARS-CoV-2 variants of concern
28 (B.1.1.7, P.1, B.1.351 and B.1.617.2) were obtained. The vaccine elicited neutralizing mAbs
29 form 8 distinct competition groups and bind epitopes overlapping with neutralizing mAbs
30 elicited following SARS-CoV-2 infection. AZD1222 elicited mAbs are more mutated than mAbs
31 isolated from convalescent donors 1-2 months post infection. Spike reactive IgG+ B cells were
32 still detectable 9-months post boost. These findings give molecular insights into AZD1222
33 elicited antibody response.

34

35

36 **Introduction**

37 The SARS-CoV-2 encoded Spike glycoprotein is the key target for neutralizing
38 antibodies (nAbs) generated in response to natural infection. The Spike trimer consists of two
39 subunits, S1, that is required for interaction with the ACE-2 receptor on target cells, and S2
40 that orchestrates membrane fusion. Many monoclonal antibodies (mAbs) have been isolated
41 from SARS-CoV-2 infected individuals allowing identification of key neutralizing epitopes on
42 Spike (Andreano et al., 2021; Barnes et al., 2020; Brouwer et al., 2020; Graham et al., 2021;
43 Piccoli et al., 2020; Robbiani et al., 2020; Rogers et al., 2020; Seydoux et al., 2020; Tortorici
44 et al., 2020). Neutralizing epitopes are present on the receptor binding domain (RBD), the N-
45 terminal domain (NTD) of Spike and S2. RBD-specific nAbs tend to be potently neutralizing
46 and target four epitopes (Barnes et al., 2020; Dejnirattisai et al., 2021; Yuan et al., 2020b),
47 including the receptor binding motif (RBM) which interacts directly with the ACE-2 receptor.
48 Furthermore, several non-overlapping neutralizing epitopes on NTD have been identified
49 which are susceptible to sequence variation in this region (Cerutti et al., 2021; Graham et al.,
50 2021; McCallum et al., 2021; Suryadevara et al., 2021). SARS-CoV-2 infection also generates
51 a large proportion of non-neutralizing antibodies of which the biological function is not fully
52 understood (Anderson et al., 2021; Beaudoin-Bussi eres, 2021; Li et al., 2021). Combined,
53 studying the antibody response to SARS-CoV-2 infection has generated an antigenic map of
54 the Spike surface (Corti et al., 2021; Dejnirattisai et al., 2021).

55 Following the emergence of SARS-CoV-2 in the human population, vaccines against
56 COVID-19 have been rapidly developed. Most licenced vaccines use, or encode, a SARS-
57 CoV-2 Spike antigen to elicit both humoral and cellular responses and many have shown
58 remarkable efficacy in Phase III trials (Baden et al., 2021; Polack et al., 2020; Voysey et al.,
59 2021). However, there are concerns that vaccine efficacy could be reduced against newly
60 emerging SARS-CoV-2 variants of concern (VOC), in particular against the alpha (B.1.1.7),
61 beta (B.1.351), gamma (P.1) and delta (B.1.617.2) variants which harbour mutations
62 throughout Spike. Serum neutralizing activity against viral variants has been reported in many
63 double vaccinated individuals, albeit at a reduced potency (Alter et al., 2021; Collier et al.,

64 2021; Edara et al., 2021; Monin et al., 2021; Supasa et al., 2021; Wang et al., 2021d; Zhou
65 and al, 2021). Despite this reduction, real-world data shows current COVID-19 vaccines are
66 still highly effective in preventing severe disease and hospitalizations in locations where
67 SARS-CoV-2 variants of concern are prevalent (Emary et al., 2021; Lopez Bernal et al., 2021;
68 Madhi et al., 2021).

69 Whilst the antibody response to COVID-19 vaccination has been studied extensively
70 at the polyclonal level using immune sera (Alter et al., 2021; Collier et al., 2021; Dejnirattisai
71 et al., 2021; Edara et al., 2021; Emary et al., 2021; Monin et al., 2021; Supasa et al., 2021;
72 Wall et al., 2021; Wang et al., 2021d; Zhou and al, 2021), little has been reported on the
73 antibody response at the monoclonal level (Amanat et al., 2021; Andreano, 2021; Cho, 2021;
74 Wang et al., 2021d). To address this paucity of information, we isolated a panel of 44 anti-
75 SARS-CoV-2 monoclonal antibodies (mAbs) from an individual (VA14) who had received 2-
76 doses of the AZD1222 (ChAdOx1 nCoV-19) vaccine at a 12-week interval (**Figure 1A**). The
77 AZD1222 vaccine is a replication-defective chimpanzee adenovirus-vectored vaccine
78 expressing the full-length Wuhan SARS-CoV-2 spike glycoprotein gene (Ramasamy et al.,
79 2021; Voysey et al., 2021). Even though low serum neutralization titres ($ID_{50} \sim 100$) were
80 detected in VA14 at 4-months post vaccine booster, nAbs were isolated which displayed
81 potent cross-neutralizing activity against SARS-CoV-2 viral variants of concern (IC_{50} values
82 as low as $0.003 \mu\text{g/mL}$). The AZD1222 vaccine elicited NTD- and RBD-specific nAbs that bind
83 epitopes overlapping with nAbs generated following natural infection. Assessment at 9-months
84 post vaccine booster revealed the presence of Spike reactive IgG+ B cells despite
85 undetectable neutralization. These data suggest that although plasma neutralization may be
86 sub-optimal for protection from infection, memory B cells may be sufficient to provide rapid
87 recall responses to protect from serious illness/hospitalizations upon re-infection.

88

89 **Results**

90 **Serum neutralizing activity following AZD1222 vaccination**

91 Plasma and peripheral blood mononuclear cells (PBMC) were isolated from donor
92 VA14 (23 years, white male) at 4-months (timepoint 1, TP1) and 9-months (timepoint 2, TP2)
93 after receiving two doses of the AZD1222 vaccine at a 12-week interval (**Figure 1A**). VA14
94 reported no previous SARS-CoV-2 infection (based on regular PCR testing), did not have N-
95 specific IgG in their plasma at the time of sampling, and was therefore presumed to be SARS-
96 CoV-2 naïve. Presence of IgG to Spike was determined by ELISA (**Figure 1B**) and a semi-
97 quantitative ELISA measured 0.39 and 0.17 $\mu\text{g/mL}$ of Spike IgG at TP1 and TP2, respectively.

98 Plasma neutralizing activity was measured using an HIV-1 (human immunodeficiency
99 virus type-1)-based virus particles, pseudotyped with Spikes of SARS-CoV-2 variants of
100 concern, including AZD1222 matched Spike (Wuhan-1, WT), and VOCs B.1.1.7, P.1, B.1.351
101 and B.1.617.2, and a HeLa cell-line stably expressing the ACE2 receptor (Graham et al., 2021;
102 Seow et al., 2020). Overall, neutralization titres at 4-months post vaccine boost (TP1) were
103 low. ID_{50}S of ~ 100 were measured against WT and P.1 but were reduced against B.1.1.7,
104 B.1.351 and B.1.351 (**Figure 1C**). Although weak binding to Spike was observed at TP2,
105 neutralization was not detected at a serum dilution of 1:20 (**Figure 1D**).

106

107 **Spike reactive B cells detected up to one year following AZD1222 vaccination**

108 Next, we determined the percentage of RBD or Spike reactive IgG expressing B cells
109 at 4- and 9-months post vaccine booster using flow cytometry (**Figure 1E and Figure S1A-**
110 **D**). 0.25% of IgG+ B cells were Spike reactive and 0.06% were RBD reactive at 4-months post
111 vaccine booster. Despite the undetectable neutralization by sera at 9-months post vaccine
112 booster, 0.27% of IgG+ B cells were Spike reactive.

113

114 **AZD1222 vaccination elicits antibodies targeting epitopes on NTD, RBD, S2 and Spike**

115 RBD or Spike reactive B cells at 4-months post vaccine booster were sorted into
116 individual wells and the antibody heavy and light chain genes rescued by reverse transcription
117 followed by nested PCR using gene-specific primers (Graham et al., 2021). Variable regions
118 were ligated into IgG1 heavy and light chain expression vectors using Gibson assembly and

119 directly transfected into HEK 293T/17 cells. Crude supernatants containing IgG were used to
120 confirm specificity to Spike and the variable heavy and light regions of Spike reactive mAbs
121 were sequenced. In total, 44 Spike reactive mAbs were isolated from VA14.

122 Binding to Spike, S1, RBD, NTD and S2 was determined by ELISA and used to identify
123 the domain-specificity of each mAb (**Figure 2A**). Of the 40 mAbs isolated using the stabilized
124 Spike sorting antigen, 45% (18/40) bound RBD, 35% (14/40) bound NTD, 17.5% (7/40) bound
125 S2 and 2.5% (1/40) bound Spike only (**Figure 2B**). A further four RBD specific mAbs were
126 isolated using the RBD sorting probe. A similar distribution between mAbs targeting RBD,
127 NTD and S2 was seen for mAbs isolated from convalescent donors 6-8 weeks post onset of
128 symptoms (POS) (Graham et al., 2021).

129

130 **AZD1222 vaccination elicits neutralizing and non-neutralizing antibodies against** 131 **epitopes across the full Spike**

132 Neutralizing activity of mAbs was initially measured using HIV-1 virus particles
133 pseudotyped with SARS-CoV-2 Spike encoded by the AZD1222 vaccine. Twenty six of 44
134 mAbs (59.1%) displayed neutralizing activity of which 21/26 (80.8%) were RBD-specific, 4/26
135 (15.5%) were NTD-specific and 1/26 (3.8%) only bound Spike (**Figure 2B**). None of the S2-
136 specific nAbs showed neutralizing activity. 95.5% of RBD-specific mAbs and 38.6% of NTD-
137 specific mAbs had neutralizing activity (**Figure 2B**). Neutralization potency against wild-type
138 Spike ranged from 0.025 – 7.3 $\mu\text{g/mL}$. As previously reported for natural infection, RBD-
139 specific nAbs had a lower geometric mean IC_{50} compared to NTD-specific nAbs (**Figure 2C**)
140 (Graham et al., 2021; Liu et al., 2020).

141

142 **AZD1222 elicited mAbs are more highly mutated than mAbs from natural infection**

143 The heavy and light chain variable regions of Spike reactive mAbs were sequenced
144 and the germline usage and level of somatic hypermutation (SHM) determined using IMGT
145 (Brochet et al., 2008). An average 4.9% and 2.8% divergence from V_H and V_L germlines was
146 observed at the nucleotide level for AZD1222 elicited mAbs (**Figure 3A**), which is higher than

147 mAbs isolated in our previous study from convalescent individuals 3-8 weeks post onset of
148 symptoms (1.9% and 1.4% for V_H and V_L respectively) (Graham et al., 2021). Three pairs of
149 related clones were identified (**Figure S2A**).

150 Germline gene usage and divergence from germline of both neutralizing and non-
151 neutralizing AZD1222 mAbs were compared to a database of SARS-CoV-2 specific mAbs
152 isolated from convalescent individuals (n = 1292) (Raybould et al., 2021) as well as paired
153 heavy and light chains of IgG B cell receptors (BCR) from blood of CD19+ B cells from healthy
154 individuals representative of circulating IgG expressing B cell repertoire (n = 862) (Siu, 2021).
155 As the SARS-CoV-2 mAb database only included amino acid sequences for some mAbs,
156 divergence from germline was determined at the amino acid level (which correlated well with
157 nucleotide divergence (**Figure S2B**)). AZD1222 elicited mAbs from donor VA14 had a
158 statistically higher amino acid mutation (V_H 9.2% and V_L 6.1%) compared to mAbs isolated
159 from SARS-CoV-2 convalescent donors (V_H 4.2% and V_L 3.0%) but had a similar level to B
160 cell receptors from healthy subjects (V_H 10.9% and V_L 8.0%) (**Figure 3B&C**). Similar
161 differences in mutation levels were observed for both neutralizing and non-neutralizing
162 antibodies (**Figure S2C**).

163 An enrichment in VH3-30 and VH3-53 germline usage was observed for both SARS-
164 CoV-2 infection and AZD1222 elicited mAbs similar to that seen for mRNA elicited mAbs
165 (Wang et al., 2021d) (**Figure 3D**). 3/21 RBD-specific nAbs used the VH3-53/3-66 germlines
166 which are common amongst nAbs that directly bind the ACE2 binding site on Spike (Barnes
167 et al., 2020; Graham et al., 2021; Kim et al., 2021; Robbiani et al., 2020; Yuan et al., 2020c).
168 An enrichment of VH4-34 and VH4-59 germline use was observed for AZD1222 elicited mAbs
169 only. 11/44 (25.0%) and 8/44 (18.2%) mAbs used VK3-20 and VK1-39 light chains,
170 respectively (**Figure 3E**).

171

172 **AZD1222 elicited nAbs bind epitopes overlapping with nAbs generated in response to**
173 **SARS-CoV-2 infection**

174 To gain insight into the epitopes targeted by the AZD1222 elicited nAbs, competition
175 ELISAs with trimeric Spike and previously characterized nAbs isolated from SARS-CoV-2
176 infected individuals were performed. The panel of competing antibodies encompassed four
177 RBD-, two NTD- and 1 Spike-only competition groups (Graham et al., 2021) (**Figures 4A-B**).
178 Additionally, the ability of nAbs to inhibit the interaction between Spike and the ACE2 receptor
179 was determined by flow cytometry (**Figure 4D**).

180 Four RBD neutralizing antibody classes have been previously identified and
181 characterized (Barnes et al., 2020; Yuan et al., 2020b). nAbs that neutralize by binding to the
182 receptor binding motif (RBM) (equivalent to RBD Class 1) (Barnes et al., 2020; Dejnirattisai et
183 al., 2021; Yuan et al., 2020a) commonly use the VH3-53 or VH3-66 germ lines. As expected,
184 the three VH3-53/VH3-66 VA14 nAbs competed with the Group 3 (RBD Class 1) infection
185 nAbs as well as competing strongly for ACE-2 binding (**Figure 4D**). Group 3 nAbs were most
186 potent at neutralizing the matched vaccine strain (Wuhan-1) (**Figure 4C**).

187 The majority of RBD-specific nAbs isolated from VA14 (13/20) competed with the
188 Group 4 (RBD Class 3) RBD infection nAbs (**Figure 4A**) and included both potent and modest
189 neutralizing Abs with varying degrees of ACE2 competition (**Figure 4C-D**). Five VA14 nAbs
190 competed with Group 1 (RBD Class 4) RBD infection nAbs and showed a wide range of
191 potencies and levels of ACE2 competition. Only one VA14 nAb (VA14_26) competed with
192 Group 2 (RBD Class 2) RBD infection nAbs which also competed strongly with ACE2.

193 NTD mAbs formed three competition groups (**Figure 4B**). Non-neutralizing mAbs
194 VA14_25 and VA14_58 competed with NTD Group 6 nAbs including P008_056 which has
195 been shown to bind NTD adjacent to the β -sandwich fold (Rosa et al., 2021b). These two
196 nAbs did not inhibit Spike binding to ACE2 (**Figure 4D**). nAbs VA14_21 and VA14_22
197 competed with NTD Group 5 nAbs and showed 51-58% inhibition of Spike binding to ACE2.
198 Two NTD nAbs (Group 8) did not compete with any of the infection NTD-specific nAbs or
199 prevent ACE2 binding.

200 The S-only binding nAb VA14_47 competed with P008_060 (Group 7) (**Figure 4B**),
201 the only other S-only infection nAb, and showed 59% inhibition of Spike binding to ACE2

202 **(Figure 4D)**. P008_060 has been shown to bind a neutralizing epitope on the SD1 domain
203 *(manuscript in preparation)*.

204

205 **AZD1222 elicited nAbs cross-neutralize SARS-CoV-2 variants of concern.**

206 Assessing the cross-neutralizing activity of nAbs isolated from SARS-CoV-2
207 convalescent donors has revealed that Spike mutations in VOCs selectively hinder
208 neutralizing activity of specific nAb classes (Graham et al., 2021; Wang et al., 2021a; Wang
209 et al., 2021b; Wang et al., 2021c; Wibmer et al., 2021). Therefore, we measured the
210 neutralization potency of AZD1222 elicited nAbs against SARS-CoV-2 variants of concern,
211 including B.1.1.7 (alpha), B.1.351 (beta), B.1.617.2 (delta) and P.1 (gamma) and compared
212 this to nAbs isolated following natural infection (Graham et al., 2021). Spike proteins from
213 these VOCs encode mutations in RBD, NTD and S2 (**Figure 5A**). Some RBD mutations are
214 shared between multiple variants, e.g. B.1.1.7, P.1 and B.1.351 all share an N501Y mutation,
215 and P.1 and B.1.351 share an E484K mutation and a mutation at K417. In contrast, NTD
216 mutations vary considerably between VOCs and include both amino acid mutations and
217 deletions. Although a reduction in neutralization potency was observed for some AZD1222
218 nAbs, RBD- and NTD-specific nAbs with potent cross-neutralization against all VOCs were
219 identified (**Figure 5B&C**).

220 All Group 3, several Group 4 (VA14_33, VA14_36, VA14R_38) and one Group 1
221 (VA14R_39) RBD-specific nAbs potently neutralized all five variants at IC₅₀s below 0.09 µg/mL
222 (**Figure 5B**). Several nAbs showed enhanced neutralization of VOCs compared to wild-type.
223 Comparing nAbs elicited following infection (Graham et al., 2021) and vaccination, infection
224 nAbs showed a greater sensitivity to Spike mutations in VOCs. Cross-neutralization of nAbs
225 in RBD Groups 1, 2 and 3 was observed for AZD1222 nAbs, whilst some infection nAbs in
226 these competition groups showed greatly reduced neutralization of VOCs P.1 and B.1.351
227 which both share the E484K mutation. RBD Group 4 mAbs varied in their neutralization of
228 VOCs. 6/13 nAbs showed cross-neutralizing activity. The remaining 7 showed a >3-fold
229 reduction in neutralization against at least one VOC with neutralizing against B.1.351 and

230 B.1.617.2 being most greatly reduced. Despite some RBD nAbs showing a decreased
231 neutralisation against VOCs, binding to variant RBD in ELISA was retained for most nAbs
232 except Group 4 nAbs VA14_19 and VA14_50 (**Figure S3A**) indicating that binding does not
233 always correlate with neutralization.

234 Considering the geometric mean IC₅₀ values, NTD-specific nAbs were most potent at
235 neutralizing the B.1.1.7 VOC. However, the three NTD-competition groups showed differential
236 sensitivities towards the other four SARS-CoV-2 variants (**Figure 5C**). For example, Group 5
237 NTD nAbs had either reduced or lacked neutralization of P.1 and B.1.617.2, whereas Group
238 8 NTD nAbs VA14_16 and VA14_68 maintained potent neutralization of B.1.617.2. NTD-
239 specific nAb, VA14_16, had broad reactivity neutralizing all variants with an IC₅₀ <0.14 µg/mL
240 and is the only cross-neutralizing NTD-specific nAbs reported thus far (McCallum et al., 2021).
241 Interestingly, two NTD-specific mAbs that had shown no neutralizing activity against WT
242 pseudotyped virus, neutralized both B.1.1.7 and P.1 (**Figure 5C**). The differences in
243 neutralization of VOCs by NTD-specific nAbs were reflected in their binding to S1 of VOCs by
244 ELISA (**Figure S3B**).

245 The S-only reactive nAbs elicited by vaccination did not neutralize any of the SARS-
246 CoV-2 variants (**Figure 5D**). In contrast, the infection elicited S-only nAb retained modest
247 neutralization against P.1 at concentrations up to 47.7 µg/mL.

248 Overall, AZD1222 vaccine elicited nAbs showed greater resistance to Spike mutations
249 in variants of concern compared to infection elicited nAbs (**Figure 5E**).

250

251 **Discussion**

252 Efficacy of COVID-19 vaccines in the face of SARS-CoV-2 emerging viral variants will
253 be critical for control of the current pandemic. Here we studied the antibody response to the
254 AZD1222 vaccine administered with a 12-week interval at the monoclonal level. The majority
255 of studies examining immune sera from AZD1222 vaccinated individuals have revealed a
256 lower potency against B.1.1.7 (range 2.2 – 9.0-fold) (Dejnirattisai et al., 2021; Emary et al.,

257 2021; Wall et al., 2021), P.1 (2.9-fold) (Dejnirattisai et al., 2021), B.1.351 (range 4.0 – 9.0-fold)
258 (Dejnirattisai et al., 2021; Madhi et al., 2021; Zhou et al., 2021) and B.1.617.2 (range 4.3 –
259 9.0-fold) (Liu et al., 2021; Wall et al., 2021) compared to neutralization of Wuhan or D614G
260 variants. Although VA14 had a low plasma neutralizing activity ($ID_{50} \sim 1:100$) at 4-months post
261 vaccine booster, 59.1% of Spike reactive mAbs isolated from antigen-reactive B cells had
262 neutralizing activity against the matched vaccine strain, and many of these mAbs displayed
263 potent cross-neutralizing activity against current SARS-CoV-2 VOCs. RBD and NTD were the
264 predominant targets for neutralizing antibodies (80.8% and 15.5% of nAbs, respectively).
265 Importantly, we identified RBD-specific nAbs from each of the four competition groups, and
266 NTD-specific nAbs, that cross-neutralized all VOCs. The polyclonal nature of the nAb
267 response elicited by AZD1222 vaccination will likely help limit full vaccine escape in the face
268 of emerging Spike mutations.

269 Competition ELISAs revealed that nAbs elicited by AZD1222 target overlapping
270 epitopes of nAbs elicited from natural SARS-CoV-2 infection. However, despite similar
271 antibody footprints, vaccine elicited nAbs from RBD competition Groups 2 and 3 showed
272 greater neutralization breadth than those elicited from natural infection. This was also
273 apparent for some NTD-specific nAbs. This increased neutralization breadth is likely due to
274 the increased divergence from germline in AZD1222 elicited nAbs (isolated 4-months post
275 booster) compared to nAbs isolated following natural infection (isolated 2 – 8 weeks post onset
276 of symptoms) leading to better tolerance of Spike mutations in VOCs. Indeed, several studies
277 have shown that increased somatic hypermutation enhances neutralization breadth against
278 VOCs (de Mattos Barbosa et al., 2021; Gaebler et al., 2021; Goel et al., 2021; Muecksch et
279 al., 2021). Analysis of the antibody-antigen interaction at the molecular level will give further
280 insight into the specific mechanisms of increased neutralization breadth for AZD1222 elicited
281 nAbs.

282 Although Spike reactive mAbs generated following AZD1222 have not previously been
283 reported, several studies report mAbs isolated following mRNA COVID-19 vaccination
284 (Amanat et al., 2021; Andreano, 2021; Cho, 2021; Wang et al., 2021d). Comparison between

285 epitopes targeted by mRNA and AZD1222 elicited nAbs showed a higher proportion of RBM
286 targeted nAbs following mRNA vaccination (Andreano, 2021; Wang et al., 2021d). A similar
287 enrichment in VH3-53 and VH3-30 germline usage was observed (Andreano, 2021; Wang et
288 al., 2021d). Despite differences in the timing of mAb isolation across reported studies, the
289 AZD1222 mAbs identified had a higher level of SHM compared to mRNA elicited mAbs and
290 showed greater cross-neutralizing activity (Andreano, 2021; Wang et al., 2021d). Possible
291 reasons for these differences include; i) timing of mAb isolation following vaccine booster, ii)
292 timing of vaccine boosters (3-week for mRNA studies vs 12-weeks in this study), iii) a
293 prolonged antigen persistence for ChAdOx vectored Spike, or iv) differences in Spike antigen
294 encoded by each vaccine (in particular, mRNA-1273 (Moderna) and BNT162b2 (Pfizer)
295 vaccines encode Spike with stabilizing mutations and a mutation that prevents S1/S2 cleavage
296 (Jackson et al., 2020; Walsh et al., 2020)). Understanding these factors will be important for
297 optimizing vaccine strategies aimed at eliciting the broadest nAb response.

298 Plasma was not available to determine the peak neutralizing response in VA14 and
299 therefore the relative decline in neutralization following AZD1222 vaccination. The neutralizing
300 antibody titre was low 4-months post vaccine boost and it is not known if this level would be
301 sufficient to provide sterilizing or near sterilizing immunity. However, the identification of B
302 cells producing antibodies with potent cross-neutralizing activity against non-overlapping
303 epitopes and the presence of Spike+ IgG+ B cells at ~1 year post vaccine prime suggests that
304 a rapid recall response will likely occur which could be sufficient to protect against severe
305 disease and/or hospitalization in the face of VOCs.

306 In summary, we show that AZD1222 vaccine administered at a 12-week interval can
307 elicit nAbs with potent cross-neutralizing activity against SARS-CoV-2 VOCs that target non-
308 overlapping epitopes on RBD and NTD. Despite undetectable plasma neutralizing activity,
309 Spike reactive IgG+ B cells are detected up to 1-year following initial vaccine priming. These
310 data provide important insights into long-term immunity and protection to SARS-CoV-2
311 emerging variants.

312

313 **Limitations of study:**

314 This study only examines mAbs isolated from one individual and therefore how
315 representative these mAbs are of the humoral immune response against AZD1222 needs to
316 be investigated further.

317

318 **EXPERIMENTAL MODEL AND SUBJECT DETAILS**

319 **Ethics.** This study used human samples from one donor collected as part of a study entitled
320 “Antibody responses following COVID-19 vaccination”. Ethical approval was obtained from the
321 King’s College London Infectious Diseases Biobank (IBD) (KDJF-110121) under the terms of
322 the IDB’s ethics permission (REC reference: 19/SC/0232) granted by the South Central –
323 Hampshire B Research Ethics Committee in 2019.

324

325 **Bacterial strains and cell culture**

326 SARS-CoV-2 pseudotypes were produced by transfection of HEK293T/17 cells and
327 neutralization activity assayed using HeLa cells stably expressing ACE2 (kind gift James E
328 Voss). Small and large scale expression of monoclonal antibodies was performed in
329 HEK293T/17 (ATCC; ATCC® CRL-11268™) and 293 Freestyle cells (Thermofisher Scientific),
330 respectively. Bacterial transformations were performed with NEB® Stable Competent *E. coli*.

331

332 **METHOD DETAILS:**

333 **Protein expression and purification.** Recombinant Spike and RBD for ELISA were
334 expressed and purified as previously described (Pickering et al., 2020; Seow et al., 2020).
335 Recombinant S1 (residues 1-530) and NTD (residues 1-310) expression and purification was
336 described in Rosa et al (Rosa et al., 2021a). S2 protein was obtained from SinoBiological (Cat
337 number: 40590-V08B).

338

339 For antigen-specific B cell sorting, Spike glycoprotein consisted of the pre-fusion S
340 ectodomain (residues 1–1138) with a GGGG substitution at the furin cleavage site (amino

341 acids 682–685), proline substitutions at amino acid positions 986 and 987, and an N-terminal
342 T4 trimerization domain. RBD consisted of amino acids 331-533. Spike and RBD were cloned
343 into a pHLsec vector containing Avi and 6xHis tags (Aricescu et al., 2006). Biotinylated Spike
344 or RBD were expressed in 1L of HEK293F cells (Invitrogen) at a density of 1.5×10^6 cells/mL.
345 To achieve *in vivo* biotinylation, 480µg of each plasmid was co-transfected with 120µg of BirA
346 (Howarth et al., 2008) and 12mg PEI-Max (1 mg/mL solution, Polysciences) in the presence
347 of 200 µM biotin (final concentration). The supernatant was harvested after 7 days and purified
348 using immobilized metal affinity chromatography and size-exclusion chromatography.
349 Complete biotinylation was confirmed via depletion of protein using avidin beads.

350

351 **ELISA (S, RBD, NTD, S2 or S1).** 96-well plates (Corning, 3690) were coated with S, S1, NTD,
352 S2 or RBD at 3 µg/mL overnight at 4°C. The plates were washed (5 times with PBS/0.05%
353 Tween-20, PBS-T), blocked with blocking buffer (5% skimmed milk in PBS-T) for 1 h at room
354 temperature. Serial dilutions of plasma, mAb or supernatant in blocking buffer were added
355 and incubated for 2 hr at room temperature. Plates were washed (5 times with PBS-T) and
356 secondary antibody was added and incubated for 1 hr at room temperature. IgM was detected
357 using Goat-anti-human-IgM-HRP (horseradish peroxidase) (1:1,000) (Sigma: A6907) and IgG
358 was detected using Goat-anti-human-Fc-AP (alkaline phosphatase) (1:1,000) (Jackson: 109-
359 055-098). Plates were washed (5 times with PBS-T) and developed with either AP substrate
360 (Sigma) and read at 405 nm (AP) or 1-step TMB (3,3',5,5'-Tetramethylbenzidine) substrate
361 (Thermo Scientific) and quenched with 0.5 M H₂SO₄ before reading at 450 nm (HRP).

362

363 **Fab/Fc ELISA.** 96-well plates (Corning, 3690) were coated with goat anti-human Fc IgG
364 antibody at 3 µg/mL overnight at 4°C. The above protocol was followed. The presence of IgG
365 in supernatants was detected using Goat-anti-human-Fc-AP (alkaline phosphatase) (1:1,000)
366 (Jackson: 109-055-098).

367

368 **IgG digestion to generate F(ab')₂.** IgG were incubated with IdeS (Dixon, 2014) (4 µg of IdeS
369 per 1 mg of IgG) in PBS for 1 hour at 37 °C. The Fc and IdeS A were removed using a mix of
370 Protein A Sepharose® Fast Flow (250 µL per 1 mg digested mAb; GE Healthcare Life
371 Sciences) and Ni Sepharose™ 6 Fast Flow (50 µL per 1 mg digested mAb; GE Healthcare
372 Life Sciences) which were washed twice with PBS before adding to the reaction mixture. After
373 exactly 10 minutes the beads were removed from the F(ab')₂-dilution by filtration in Spin-X
374 tube filters (Costar®) and the filtrate was concentrated in Amicon® Ultra Filters (10k, Millipore).
375 Purified F(ab')₂ fragments were analysed by SDS-PAGE.

376

377 **F(ab')₂ and IgG competition ELISA.** 96-well half area high bind microplates (Corning®) were
378 coated with S-protein at 3µg/mL in PBS overnight at 4 °C. Plates were washed (5 times with
379 PBS/0.05% Tween-20, PBS-T) and blocked with 5% milk in PBS/T for 2 hr at room
380 temperature. Serial dilutions (5-fold) of F(ab')₂, starting at 100-molar excess of the IC₈₀ of S
381 binding, were added to the plates and incubated for 1 hr at room temperature. Plates were
382 washed (5 times with PBS-T) before competing IgG was added at their IC₈₀ of S binding and
383 incubated at room temperature for 1 hr. Plates were washed (5 times with PBS-T) and Goat-
384 anti-human-Fc-AP (alkaline phosphatase) (1:1,000) (Jackson: 109-055-098) was added and
385 incubated for 45 minutes at room temperature. The plates were washed (5 times with PBS-T)
386 and AP substrate (Sigma) was added. Optical density was measured at 405 nm in 5-minute
387 intervals. The percentage competition was calculated as the reduction in IgG binding in the
388 presence of F(ab')₂ (at 100-molar excess of the IC₈₀) as a percentage of the maximum IgG
389 binding in the absence of F(ab')₂. Competition groups were determined using Ward2 clustering
390 (R, Complex Heatmap package (Gu et al., 2016)) for initial analysis and Groups were then
391 arranged by hand according to binding epitopes.

392

393 **Semi-quantitative ELISA.** In 96-well plates (Corning, 3690), 10 columns were coated with
394 SARS-CoV-2 Spike at 3 µg/mL in PBS, with the remaining 2 columns coated with Goat anti-
395 Human IgG F(ab')₂ at 1:1000 dilution, and incubated overnight at 4°C. The plates were washed

396 (5 times with PBS/0.05% Tween-20, PBS-T) and blocked with blocking buffer (5% skimmed
397 milk in PBS-T) for 1 h at room temperature. Serial dilutions of serum and a known
398 concentrations of IgG standard (in blocking buffer) were added to the Spike coated and
399 standard curve columns, respectively. After 2 h incubation at room temperature, plates were
400 washed 5 times with PBS-T. Secondary antibody, goat-anti-human-Fc-AP, was added at
401 1:1000 dilution in blocking buffer and incubated for 1 h at room temperature. Plates were
402 washed 5 times with PBS-T and developed with AP substrate (Sigma). Absorbance was
403 measured at 405 nm. Antigen-specific serum IgG was quantified by averaging values
404 interpolated from a standard curve of IgG standard using four-parameter logistic regression
405 curve fitting (Rees-Spear et al., 2021).

406

407 **SARS-CoV-2 pseudotyped virus preparation.** Pseudotyped HIV-1 virus incorporating either
408 the SARS-Cov-2 Wuhan, B.1.1.7, P.1, B.1.351, B.1.617.2 full-length Spike were produced in
409 a 10 cm dish seeded the day prior with 5×10^6 HEK293T/17 cells in 10 mL of complete
410 Dulbecco's Modified Eagle's Medium (DMEM-C, 10% fetal bovine serum (FBS) and 1%
411 Pen/Strep (100 IU/mL penicillin and 100 mg/mL streptomycin)). Cells were transfected using
412 90 mg of PEI-Max (1 mg/mL, Polysciences) with: 15 μ g of HIV-luciferase plasmid, 10 μ g of
413 HIV 8.91 gag/pol plasmid (Zufferey et al., 1997) and 5 μ g of SARS-CoV-2 spike protein
414 plasmid (Grehan et al., 2015; Thompson et al., 2020). Pseudotyped virus was harvested after
415 72 hours, filtered through a 0.45mm filter and stored at -80°C until required.

416

417 **Neutralization assay with SARS-CoV-2 pseudotyped virus.** Neutralization assays were
418 conducted as previously described (Carter et al., 2020; Monin et al., 2021; Seow et al., 2020).
419 Serial dilutions of serum samples (heat inactivated at 56°C for 30mins) or mAbs were prepared
420 with DMEM-C media and incubated with pseudotyped virus for 1-hour at 37°C in 96-well
421 plates. Next, HeLa cells stably expressing the ACE2 receptor (provided by Dr James Voss,
422 Scripps Research, La Jolla, CA) were added (12,500 cells/50 μ L per well) and the plates were
423 left for 72 hours. The amount of infection was assessed in lysed cells with the Bright-Glo

424 luciferase kit (Promega), using a Victor™ X3 multilabel reader (Perkin Elmer). Measurements
425 were performed in duplicate and duplicates used to calculate the ID₅₀.

426

427 **Antigen-specific B cell sorting.** Fluorescence-activated cell sorting of cryopreserved
428 PBMCs was performed on a BD FACS Melody as previously described (Graham et al., 2021).
429 Sorting baits (SARS-CoV-2 Spike and RBD) was pre-complexed with the streptavidin
430 fluorophore at a 1:4 molar ratio prior to addition to cells. PBMCs were stained with live/dead
431 (fixable Aqua Dead, Thermofisher), anti-CD3-APC/Cy7 (Biolegend), anti-CD8-APC-Cy7
432 (Biolegend), anti-CD14-BV510 (Biolegend), anti-CD19-PerCP-Cy5.5 (Biolegend), anti-IgM-
433 PE (Biolegend), anti-IgD-Pacific Blue (Biolegend) and anti-IgG-PeCy7 (BD) and Spike-
434 Alexa488 (Thermofisher Scientific, S32354) and Spike-APC (Thermofisher Scientific, S32362)
435 or RBD-Alexa488 and RBD-APC. Live CD3⁺CD8⁻CD14⁻CD19⁺IgM⁻IgD⁻IgG⁺Spike⁺Spike⁺ or
436 CD3⁺CD8⁻CD14⁻CD19⁺IgM⁻IgD⁻IgG⁺RBD⁺RBD⁺ cells were sorted using a BD FACS Melody
437 into individual wells containing RNase OUT (Invitrogen), First Strand SuperScript III buffer,
438 DTT and H₂O (Invitrogen) and RNA was converted into cDNA (SuperScript III Reverse
439 Transcriptase, Invitrogen) using random hexamers (Bioline Reagents Ltd) following the
440 manufacturer's protocol.

441

442 **Full-length antibody cloning and expression.** The human Ab variable regions of heavy and
443 kappa/lambda chains were PCR amplified using previously described primers and PCR
444 conditions (Scheid et al., 2009; Tiller et al., 2008; von Boehmer et al., 2016). PCR products
445 were purified and cloned into human-IgG (Heavy, Kappa or Lambda) expression plasmids(von
446 Boehmer et al., 2016) using the Gibson Assembly Master Mix (NEB) following the
447 manufacturer's protocol. Gibson assembly products were directly transfected into HEK-293T
448 cells and transformed under ampicillin selection. Ab supernatants were harvested 3 days after
449 transfection and IgG expression and Spike-reactivity determined using ELISA. Ab variable
450 regions of heavy-light chain pairs that generated Spike reactive IgG were sequenced by
451 Sanger sequencing.

452

453 **IgG expression and purification.** Ab heavy and light plasmids were co-transfected at a 1:1
454 ratio into HEK-293F cells (ThermoFisher) using PEI Max (1 mg/mL, Polysciences, Inc.) at a
455 3:1 ratio (PEI Max:DNA). Ab supernatants were harvested five days following transfection,
456 filtered and purified using protein G affinity chromatography following the manufacturer's
457 protocol (GE Healthcare).

458

459 **ACE2 competition measured by flow cytometry.** To prepare the fluorescent probe,
460 Streptavidin-APC (ThermoFisher Scientific, S32362) was added to biotinylated SARS-CoV-2
461 Spike (3.5 times molar excess of Spike) on ice. Additions were staggered over 5 steps with
462 30 min incubation times between each addition. Purified mAbs were mixed with PE conjugated
463 SARS-CoV-2 S in a molar ratio of 4:1 in FACS buffer (2% FBS in PBS) on ice for 1 h. HeLa-
464 ACE2 and HeLa cells were washed once with PBS and detached using PBS containing 5mM
465 EDTA. Detached cells were washed and resuspended in FACS buffer. 0.5 million HeLa-ACE2
466 cells were added to each mAb-Spike complex and incubated on ice for 30 m. The cells were
467 washed with PBS and resuspended in 1 mL FACS buffer with 1 μ L of LIVE/DEAD Fixable
468 Aqua Dead Cell Stain Kit (Invitrogen). HeLa-ACE2 cells alone and with SARS-CoV-2 Spike
469 only were used as background and positive controls, respectively. The geometric mean
470 fluorescence for PE was measured from the gate of singlet and live cells. The ACE2 binding
471 inhibition percentage was calculated as described previously (Graham et al., 2021; Rogers et
472 al., 2020).

473

474 **Monoclonal antibody sequence analysis.** The heavy and light chain sequences of SARS-
475 CoV-2 specific mAbs were examined using IMGT/V-QUEST
476 (http://www.imgt.org/IMGT_vquest/vquest) to identify the germline usages, percentage of
477 SHM and CDR region lengths. To remove variation introduced through cloning using mixture
478 of forward primers, 5 amino acids or 15 nucleotides were trimmed from the start and end of
479 the translated variable genes. D'Agostino & Pearson normality test, Kruskal-Wallis test with

480 Dunn's multiple comparisons post hoc test, Ordinary one-way ANOVA with Tukey's multiple
481 comparisons post hoc test and two-sided binomial tests) were performed using GraphPad
482 Prism software. Significance defined as $p < 0.0332$ (*), 0.0021 (**), 0.0002 (***) and >0.0001
483 (****).

484

485 **Acknowledgements**

486 We thank Philip Brouwer, Marit van Gils and Rogier Sanders for the Spike protein construct,
487 Peter Cherepanov for S1 proteins from VOCs, Leo James and Jakub Luptak for the N protein,
488 Wendy Barclay for providing the B.1.617.2 Spike plasmid and James Voss and Deli Huang
489 for providing the Hela-ACE2 cells.

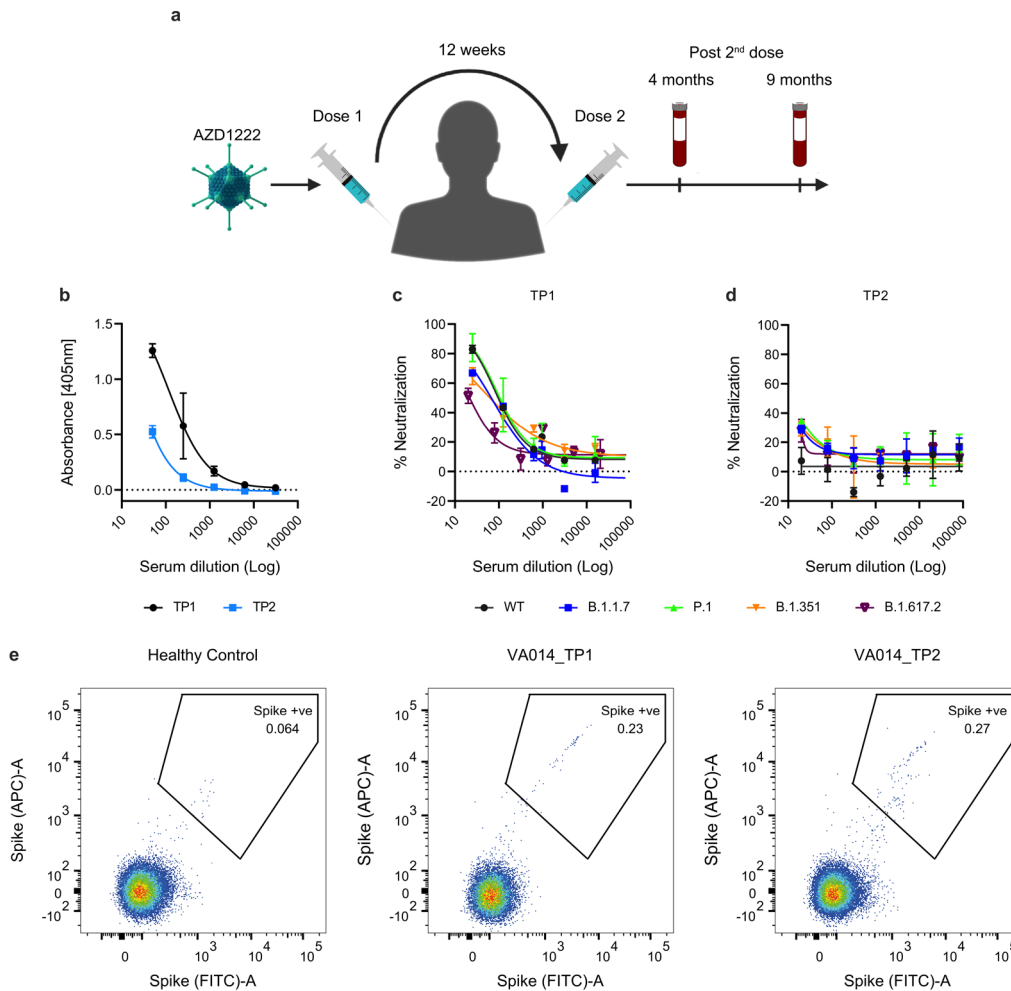
490

491 **Funding**

492 This work was funded by; Huo Family Foundation Award to MHM and KJD, MRC Genotype-
493 to-Phenotype UK National Virology Consortium (MR/W005611/1 to MHM and KJD), Fondation
494 Dormeur, Vaduz for funding equipment to KJD, Wellcome Trust Investigator Award
495 106223/Z/14/Z to MHM, and Wellcome Trust Multi-User Equipment Grant 208354/Z/17/Z to
496 M.H.M. and K.J.D. CG and SH were supported by the MRC-KCL Doctoral Training Partnership
497 in Biomedical Sciences (MR/N013700/1). DC was supported by a BBSRC CASE in
498 partnership with GlaxoSmithKline (BB/V509632/1). This work was supported by the
499 Department of Health via a National Institute for Health Research comprehensive Biomedical
500 Research Centre award to Guy's and St. Thomas' NHS Foundation Trust in partnership with
501 King's College London and King's College Hospital NHS Foundation Trust. CM and the
502 Infectious Diseases Biobank are supported by the NIHR BRC. This study is part of the
503 EDCTP2 programme supported by the European Union (grant number RIA2020EF-3008
504 COVAB) (KJD, JF, MHM). The views and opinions of authors expressed herein do not
505 necessarily state or reflect those of EDCTP. This project is supported by a joint initiative
506 between the Botnar Research Centre for Child Health and the European & Developing
507 Countries Clinical Trials Partnership (KJD and JF).

508 **Figure Legends**

509 **Figure 1: VA14 plasma neutralization and Spike reactive B cells. A)** Timeline of AZD1222
510 vaccination and blood sampling for donor VA14. **B)** Plasma IgG binding to Spike at TP1 (4-
511 months post booster) and TP2 (9-months post booster). Plasma neutralizing activity against
512 HIV-1 based virus particles, pseudotyped with the Wuhan, B.1.1.7, P.1, B.1.351 or B.1.617.2
513 Spike at **C)** TP1 and **D)** TP2. **E)** Fluorescent activated cell sorting (FACS) showing percentage
514 of CD19+IgG+ B Cells binding to SARS-CoV-2 Spike at TP1 and TP2. A healthy control PBMC
515 sample collected prior to the COVID-19 pandemic was used to measure background binding
516 to Spike. The full gating strategy and sorting of RBD specific B cells can be found in
517 **Supplementary Figure 1.**

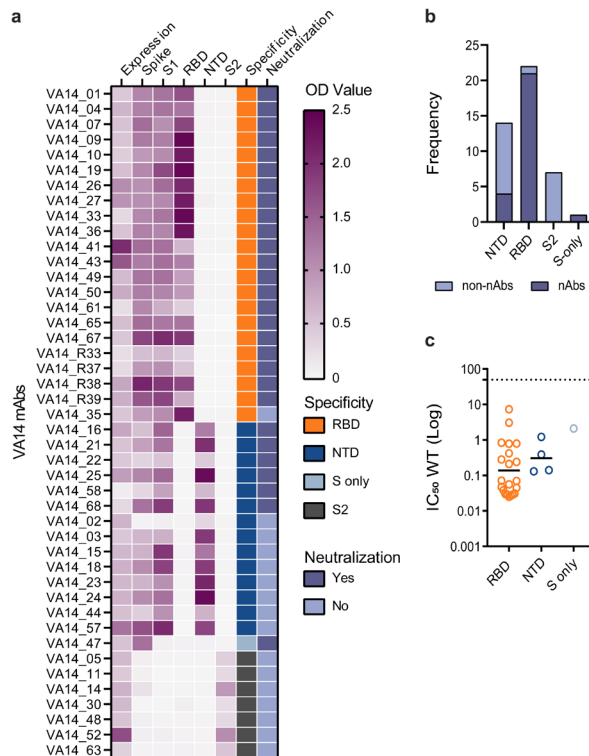


518

519

520

521 **Figure 2: AZD1222 elicits neutralizing and non-neutralizing antibodies targeting RBD,**
 522 **NTD, S1 and S2 domains of Spike. A)** Heatmap showing IgG expression level and binding
 523 to SARS-CoV-2 Spike domains, RBD, NTD, S1 and S2. The figure reports OD values from a
 524 single experiment (range 0–2.5) for undiluted supernatant from small scale transfection of 44
 525 cloned mAbs. Antigen binding was considered positive when OD at 405 nm was >0.2 after
 526 background was subtracted. SARS-CoV-2 Spike domain specificity for each antibody is
 527 indicated. Neutralization activity was measured against wild-type (Wuhan) pseudotyped virus
 528 using either small-scale purified IgG or concentrated supernatant. **B)** Frequency of
 529 neutralizing and non-neutralizing antibodies targeting either RBD, NTD, S-only or S2. Graph
 530 only includes mAbs isolated using Spike as antigen-bait for B cell sorting. **C)** Neutralization
 531 potency (IC_{50}) against wild-type (Wuhan) pseudotyped virus for mAbs targeting either RBD,
 532 NTD or non-S1. The black line represents the geometric mean IC_{50} . Related to
 533 **Supplementary Figure 2.**

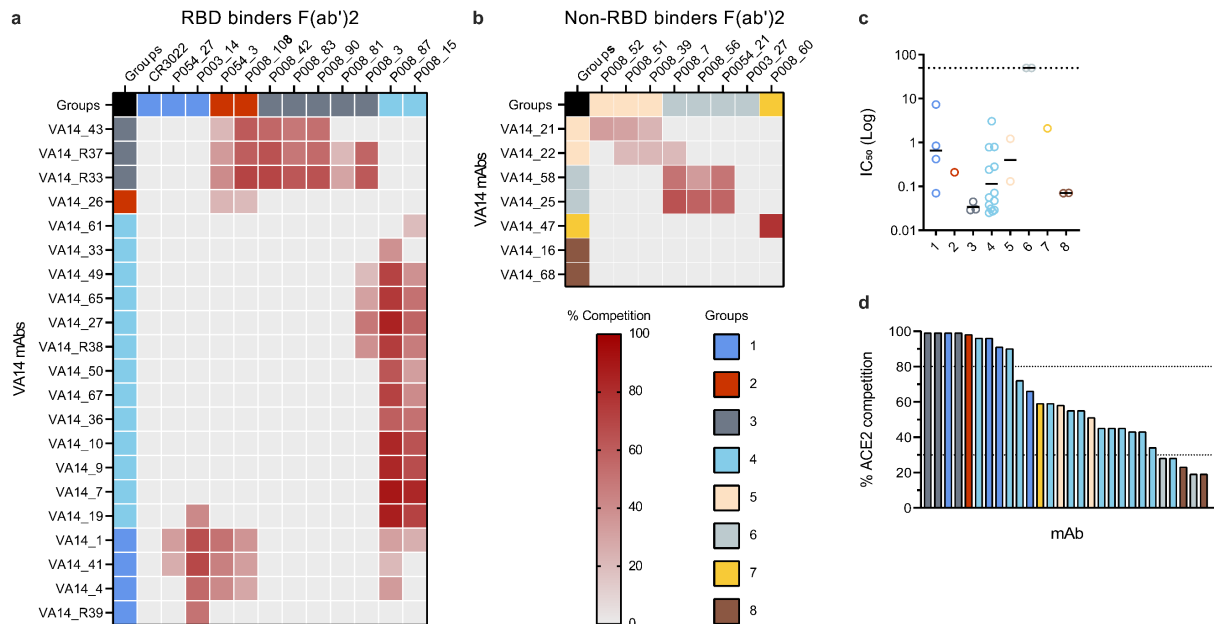


534

535

536

537 **Figure 3: AZD1222 elicited monoclonal antibodies are more mutated than those elicited**
 538 **following SARS-CoV-2 infection. A)** Truncated violin plot showing the percentage nucleotide
 539 mutation compared to germline for the VH and VL genes of Spike-reactive mAbs isolated
 540 following AZD1222. Divergence from germline (based on amino acid alignments) for **B)** VH
 541 and **C)** VL genes for Spike reactive mAbs from natural infection, AZD1222 vaccination and
 542 IgG BCRs from SARS-CoV-2 naïve individuals (Siu, 2021). D'Agostino & Pearson tests was
 543 performed to determine normality. Based on the result a Kruskal-Wallis test with Dunn's
 544 multiple comparison post hoc test was performed. * $p < 0.0332$, ** $p < 0.0021$, *** $p < 0.0002$ and
 545 **** $p < 0.0001$. Graph showing the relative abundance of **D)** VH and **E)** VL genes in mAbs elicited
 546 from AZD1222 vaccination compared to SARS-CoV-2 infection mAbs (Raybould et al., 2021)
 547 and IgG BCRs from SARS-CoV-2 naïve individuals (Siu, 2021). A two-sided binomial test was
 548 used to compare the frequency distributions. * $p < 0.0332$, ** $p < 0.0021$, *** $p < 0.0002$ and
 549 **** $p < 0.0001$. Related to **Supplementary Figure 2**.



550

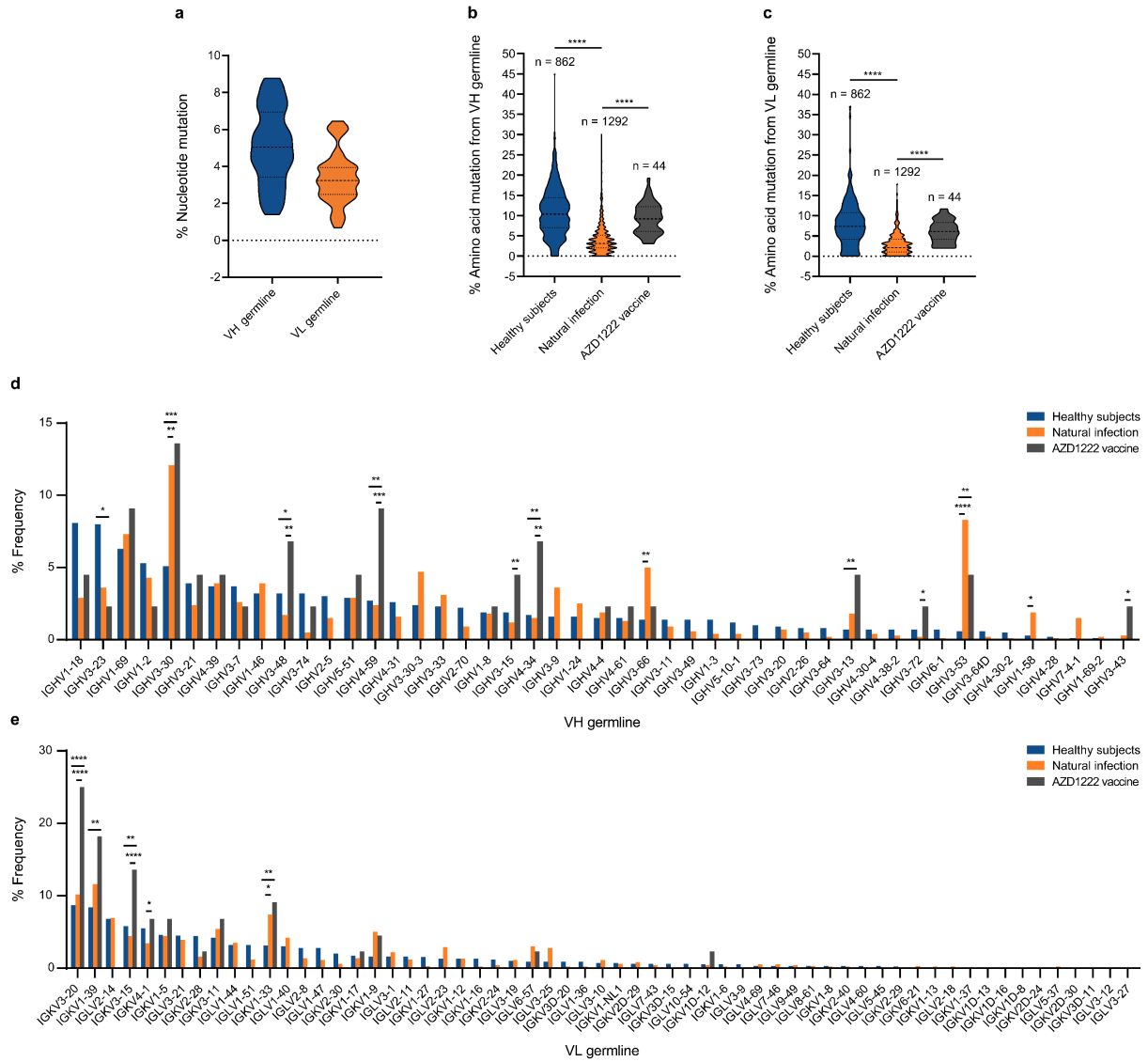
551

552

553

554

555 **Figure 4: AZD1222 nAbs target epitopes overlapping with nAbs elicited following**
556 **natural SARS-CoV-2 infection. A-B)** Competitive binding of AZD1222 and SARS-CoV-2
557 infection elicited nAbs. Inhibition of IgG binding to SARS-CoV-2 Spike by F(ab)₂' fragments
558 was measured. The percentage competition was calculated using the reduction in IgG binding
559 in the presence of F(ab')₂ (at 100-molar excess of the IC₈₀) as a percentage of the maximum
560 IgG binding in the absence of F(ab')₂. Competition was measured between **A)** RBD-specific
561 and **B)** NTD-specific/S-only nAbs. **C)** Neutralization potency (IC₅₀) of mAbs targeting either
562 RBD, NTD or non-S1 and/or in competition Groups 1–8 against SARS-CoV-2 WT
563 pseudotyped virus. Competition groups are colour coded according to the key. The black lines
564 represent the geometric mean IC₅₀ for each group. IC₅₀ values are the average of three
565 independent experiments performed in duplicate. **D)** Ability of nAbs to inhibit the interaction
566 between cell surface ACE2 and soluble SARS-CoV-2 Spike. nAbs (at 600 nM) were pre-
567 incubated with fluorescently labeled Spike before addition to HeLa-ACE2 cells. The
568 percentage reduction in mean fluorescence intensity is reported. Experiments were performed
569 in duplicate. Bars are colour coded based on their competition group.



570

571

572

573

574

575

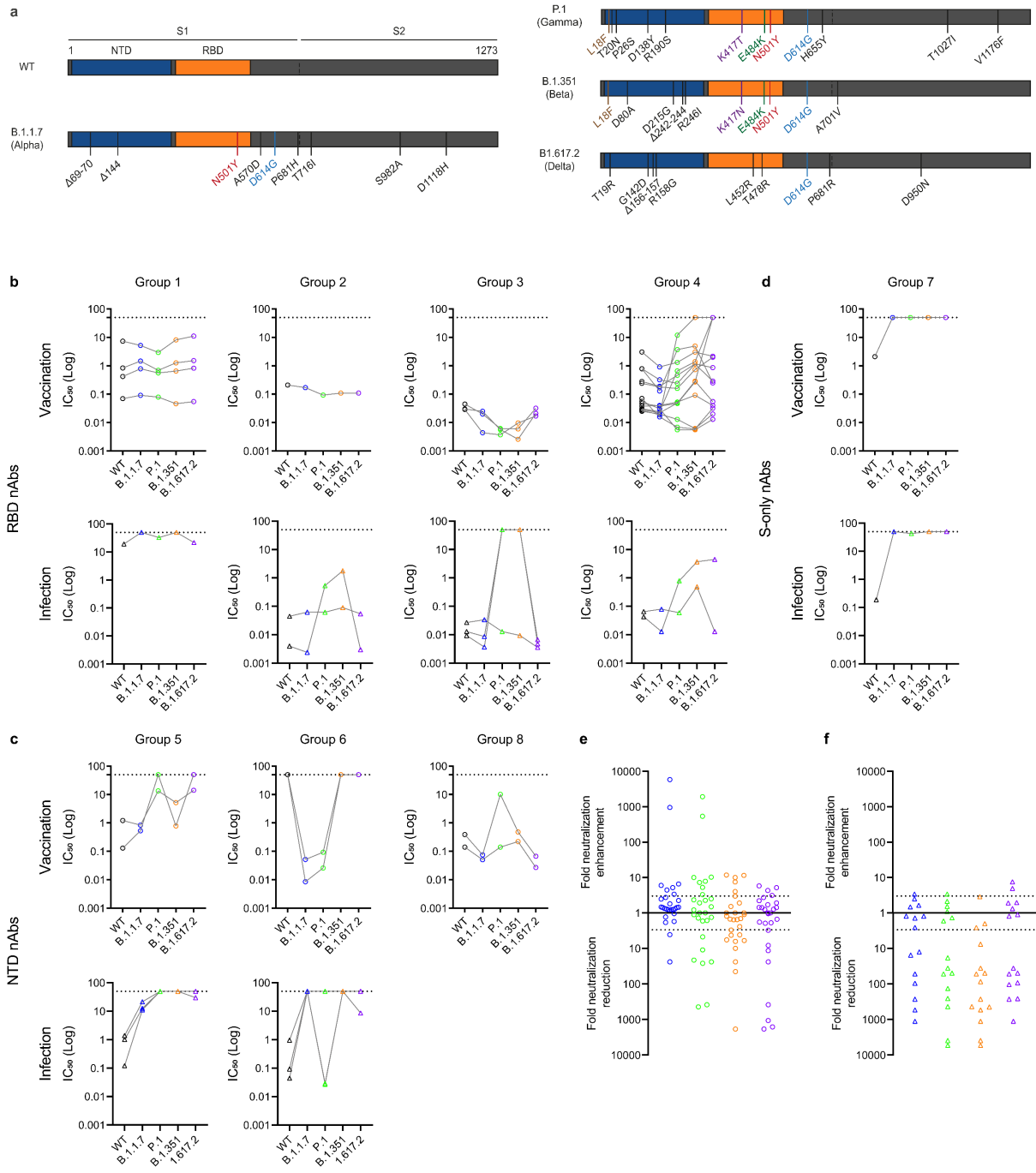
576

577

578

579

580 **Figure 5: AZD1222 generates nAbs with cross-neutralizing activity against SARS-CoV-**
581 **2 viral variants. A)** Schematic showing mutations present in the Spike of SARS-CoV-2 viral
582 variants of concern (B.1.1.7, P.1, B.1.351, B.1.617.2). **B)** Neutralization by RBD-specific nAbs
583 isolated following AZD1222 vaccination or SARS-CoV-2 infection against main variants of
584 concern. nAbs are separated by competition group (Groups 1-4). **C)** Neutralization by NTD-
585 specific nAbs isolated following AZD1222 vaccination or SARS-CoV-2 infection against main
586 variants of concern. nAbs are separated by competition group (Groups 5, 6 and 8). **D)**
587 Neutralization by S-only specific nAbs isolated following AZD1222 vaccination or SARS-CoV-
588 2 infection against main variants of concern. Fold enhancement or reduction in neutralization
589 IC_{50} against VOCs B.1.1.7, P.1, B.1.351, B.1.617.2 compared to the IC_{50} against wild-type for
590 **E)** AZD1222 elicited mAbs and **F)** infection mAbs. The dotted line indicates a 3-fold reduction
591 or enhancement in neutralization. Related to **Supplementary Figure 3 and Supplementary**
592 **Table 1.**



594 **References**

- 595 Alter, G., Yu, J., Liu, J., Chandrashekar, A., Borducchi, E.N., Tostanoski, L.H., McMahan, K.,
596 Jacob-Dolan, C., Martinez, D.R., Chang, A., *et al.* (2021). Immunogenicity of Ad26.COV2.S
597 vaccine against SARS-CoV-2 variants in humans. *Nature*.
598 Amanat, F., Thapa, M., Lei, T., Ahmed, S.M.S., Adelsberg, D.C., Carreno, J.M., Strohmeier,
599 S., Schmitz, A.J., Zafar, S., Zhou, J.Q., *et al.* (2021). SARS-CoV-2 mRNA vaccination induces
600 functionally diverse antibodies to NTD, RBD, and S2. *Cell* **184**, 3936-3948 e3910.
601 Anderson, E.M., Goodwin, E.C., Verma, A., Arevalo, C.P., Bolton, M.J., Weirick, M.E., Gouma,
602 S., McAllister, C.M., Christensen, S.R., Weaver, J., *et al.* (2021). Seasonal human coronavirus
603 antibodies are boosted upon SARS-CoV-2 infection but not associated with protection. *Cell*
604 **184**, 1858-1864 e1810.
605 Andreano, E. (2021). Hybrid immunity improves B cell frequency, antibody potency and breath
606 against SARS-CoV-2 and variants of concern. *bioRxiv*.
607 Andreano, E., Nicastrì, E., Paciello, I., Pileri, P., Manganaro, N., Piccini, G., Manenti, A.,
608 Pantano, E., Kabanova, A., Troisi, M., *et al.* (2021). Extremely potent human monoclonal
609 antibodies from COVID-19 convalescent patients. *Cell*.
610 Aricescu, A.R., Lu, W., and Jones, E.Y. (2006). A time- and cost-efficient system for high-level
611 protein production in mammalian cells. *Acta Crystallogr D Biol Crystallogr* **62**, 1243-1250.
612 Baden, L.R., El Sahly, H.M., Essink, B., Kotloff, K., Frey, S., Novak, R., Diemert, D., Spector,
613 S.A., Rouphael, N., Creech, C.B., *et al.* (2021). Efficacy and Safety of the mRNA-1273 SARS-
614 CoV-2 Vaccine. *N Engl J Med* **384**, 403-416.
615 Barnes, C.O., Jette, C.A., Abernathy, M.E., Dam, K.A., Esswein, S.R., Gristick, H.B., Malyutin,
616 A.G., Sharaf, N.G., Huey-Tubman, K.E., Lee, Y.E., *et al.* (2020). SARS-CoV-2 neutralizing
617 antibody structures inform therapeutic strategies. *Nature* **588**, 682-687.
618 Beaudoin-Bussièrès, G. (2021). An anti-SARS-CoV-2 non-neutralizing antibody with Fc-
619 effector function defines a new NTD epitope and delays neuroinvasion and death in K18-
620 hACE2 mice. *bioRxiv*.
621 Brochet, X., Lefranc, M.P., and Giudicelli, V. (2008). IMGT/V-QUEST: the highly customized
622 and integrated system for IG and TR standardized V-J and V-D-J sequence analysis. *Nucleic*
623 *Acids Res* **36**, W503-508.
624 Brouwer, P.J.M., Caniels, T.G., van der Straten, K., Snitselaar, J.L., Aldon, Y., Bangaru, S.,
625 Torres, J.L., Okba, N.M.A., Claireaux, M., Kerster, G., *et al.* (2020). Potent neutralizing
626 antibodies from COVID-19 patients define multiple targets of vulnerability. *Science* **369**, 643-
627 650.
628 Carter, M.J., Fish, M., Jennings, A., Doores, K.J., Wellman, P., Seow, J., Acors, S., Graham,
629 C., Timms, E., Kenny, J., *et al.* (2020). Peripheral immunophenotypes in children with
630 multisystem inflammatory syndrome associated with SARS-CoV-2 infection. *Nat Med*.
631 Cerutti, G., Guo, Y., Zhou, T., Gorman, J., Lee, M., Rapp, M., Reddem, E.R., Yu, J., Bahna,
632 F., Bimela, J., *et al.* (2021). Potent SARS-CoV-2 neutralizing antibodies directed against spike
633 N-terminal domain target a single supersite. *Cell Host Microbe* **29**, 819-833 e817.
634 Cho, A. (2021). Anti- SARS-CoV-2 Receptor Binding Domain Antibody Evolution after mRNA
635 Vaccination. *bioRxiv*.
636 Collier, D.A., De Marco, A., Ferreira, I., Meng, B., Datir, R., Walls, A.C., Kemp, S.S., Bassi, J.,
637 Pinto, D., Fregni, C.S., *et al.* (2021). Sensitivity of SARS-CoV-2 B.1.1.7 to mRNA vaccine-
638 elicited antibodies. *Nature*.
639 Corti, D., Purcell, L.A., Snell, G., and Veessler, D. (2021). Tackling COVID-19 with neutralizing
640 monoclonal antibodies. *Cell* **184**, 3086-3108.
641 de Mattos Barbosa, M.G., Liu, H., Huynh, D., Shelley, G., Keller, E.T., Emmer, B.T., Sherman,
642 E., Ginsburg, D., Kennedy, A.A., Tai, A.W., *et al.* (2021). IgV somatic mutation of human anti-
643 SARS-CoV-2 monoclonal antibodies governs neutralization and breadth of reactivity. *JCI*
644 *Insight* **6**.
645 Dejnirattisai, W., Zhou, D., Ginn, H.M., Duyvesteyn, H.M.E., Supasa, P., Case, J.B., Zhao, Y.,
646 Walter, T.S., Mentzer, A.J., Liu, C., *et al.* (2021). The antigenic anatomy of SARS-CoV-2
647 receptor binding domain. *Cell* **184**, 2183-2200 e2122.

- 648 Dixon, E.V. (2014). Mechanisms of immunoglobulin deactivation by *Streptococcus pyogenes*.
649 PhD Thesis.
- 650 Edara, V.V., Pinsky, B.A., Suthar, M.S., Lai, L., Davis-Gardner, M.E., Floyd, K., Flowers, M.W.,
651 Wrammert, J., Hussaini, L., Ciric, C.R., *et al.* (2021). Infection and Vaccine-Induced
652 Neutralizing-Antibody Responses to the SARS-CoV-2 B.1.617 Variants. *N Engl J Med*.
653 Emary, K.R.W., Golubchik, T., Aley, P.K., Ariani, C.V., Angus, B., Bibi, S., Blane, B., Bonsall,
654 D., Cicconi, P., Charlton, S., *et al.* (2021). Efficacy of ChAdOx1 nCoV-19 (AZD1222) vaccine
655 against SARS-CoV-2 variant of concern 202012/01 (B.1.1.7): an exploratory analysis of a
656 randomised controlled trial. *Lancet* 397, 1351-1362.
- 657 Gaebler, C., Wang, Z., Lorenzi, J.C.C., Muecksch, F., Finkin, S., Tokuyama, M., Cho, A.,
658 Jankovic, M., Schaefer-Babajew, D., Oliveira, T.Y., *et al.* (2021). Evolution of antibody
659 immunity to SARS-CoV-2. *Nature* 591, 639-644.
- 660 Goel, R.R., Painter, M.M., Apostolidis, S.A., Mathew, D., Meng, W., Rosenfeld, A.M.,
661 Lundgreen, K.A., Reynaldi, A., Khoury, D.S., Pattekar, A., *et al.* (2021). mRNA Vaccination
662 Induces Durable Immune Memory to SARS-CoV-2 with Continued Evolution to Variants of
663 Concern. *bioRxiv*.
- 664 Graham, C., Seow, J., Huettner, I., Khan, H., Kouphou, N., Acors, S., Winstone, H., Pickering,
665 S., Galao, R.P., Dupont, L., *et al.* (2021). Neutralization potency of monoclonal antibodies
666 recognizing dominant and subdominant epitopes on SARS-CoV-2 Spike is impacted by the
667 B.1.1.7 variant. *Immunity*.
- 668 Grehan, K., Ferrara, F., and Temperton, N. (2015). An optimised method for the production of
669 MERS-CoV spike expressing viral pseudotypes. *MethodsX* 2, 379-384.
- 670 Gu, Z., Eils, R., and Schlesner, M. (2016). Complex heatmaps reveal patterns and correlations
671 in multidimensional genomic data. *Bioinformatics* 32, 2847-2849.
- 672 Howarth, M., Liu, W., Puthenveetil, S., Zheng, Y., Marshall, L.F., Schmidt, M.M., Wittrup, K.D.,
673 Bawendi, M.G., and Ting, A.Y. (2008). Monovalent, reduced-size quantum dots for imaging
674 receptors on living cells. *Nat Methods* 5, 397-399.
- 675 Jackson, L.A., Anderson, E.J., Roupael, N.G., Roberts, P.C., Makhene, M., Coler, R.N.,
676 McCullough, M.P., Chappell, J.D., Denison, M.R., Stevens, L.J., *et al.* (2020). An mRNA
677 Vaccine against SARS-CoV-2 - Preliminary Report. *N Engl J Med* 383, 1920-1931.
- 678 Kim, S.I., Noh, J., Kim, S., Choi, Y., Yoo, D.K., Lee, Y., Lee, H., Jung, J., Kang, C.K., Song,
679 K.H., *et al.* (2021). Stereotypic neutralizing VH antibodies against SARS-CoV-2 spike protein
680 receptor binding domain in patients with COVID-19 and healthy individuals. *Sci Transl Med*
681 13.
- 682 Li, D., Edwards, R.J., Manne, K., Martinez, D.R., Schafer, A., Alam, S.M., Wiehe, K., Lu, X.,
683 Parks, R., Sutherland, L.L., *et al.* (2021). In vitro and in vivo functions of SARS-CoV-2
684 infection-enhancing and neutralizing antibodies. *Cell* 184, 4203-4219 e4232.
- 685 Liu, C., Ginn, H.M., Dejnirattisai, W., Supasa, P., Wang, B., Tuekprakhon, A., Nutalai, R.,
686 Zhou, D., Mentzer, A.J., Zhao, Y., *et al.* (2021). Reduced neutralization of SARS-CoV-2
687 B.1.617 by vaccine and convalescent serum. *Cell*.
- 688 Liu, L., Wang, P., Nair, M.S., Yu, J., Rapp, M., Wang, Q., Luo, Y., Chan, J.F., Sahi, V.,
689 Figueroa, A., *et al.* (2020). Potent neutralizing antibodies against multiple epitopes on SARS-
690 CoV-2 spike. *Nature* 584, 450-456.
- 691 Lopez Bernal, J., Andrews, N., Gower, C., Gallagher, E., Simmons, R., Thelwall, S., Stowe,
692 J., Tessier, E., Groves, N., Dabrera, G., *et al.* (2021). Effectiveness of Covid-19 Vaccines
693 against the B.1.617.2 (Delta) Variant. *N Engl J Med*.
- 694 Madhi, S.A., Baillie, V., Cutland, C.L., Voysey, M., Koen, A.L., Fairlie, L., Padayachee, S.D.,
695 Dheda, K., Barnabas, S.L., Bhorat, Q.E., *et al.* (2021). Efficacy of the ChAdOx1 nCoV-19
696 Covid-19 Vaccine against the B.1.351 Variant. *N Engl J Med*.
- 697 McCallum, M., Marco, A., Lempp, F., Tortorici, M.A., Pinto, D., Walls, A.C., Beltramello, M.,
698 Chen, A., Liu, Z., Zatta, F., *et al.* (2021). N-terminal domain antigenic mapping reveals a site
699 of vulnerability for SARS-CoV-2. *Cell*.
- 700 Monin, L., Laing, A.G., Munoz-Ruiz, M., McKenzie, D.R., Del Molino Del Barrio, I., Alaguthurai,
701 T., Domingo-Vila, C., Hayday, T.S., Graham, C., Seow, J., *et al.* (2021). Safety and

702 immunogenicity of one versus two doses of the COVID-19 vaccine BNT162b2 for patients with
703 cancer: interim analysis of a prospective observational study. *Lancet Oncol.*
704 Muecksch, F., Weisblum, Y., Barnes, C.O., Schmidt, F., Schaefer-Babajew, D., Wang, Z., JC,
705 C.L., Flyak, A.I., DeLaitch, A.T., Huey-Tubman, K.E., *et al.* (2021). Affinity maturation of
706 SARS-CoV-2 neutralizing antibodies confers potency, breadth, and resilience to viral escape
707 mutations. *Immunity* 54, 1853-1868 e1857.
708 Piccoli, L., Park, Y.J., Tortorici, M.A., Czudnochowski, N., Walls, A.C., Beltramello, M., Silacci-
709 Fregni, C., Pinto, D., Rosen, L.E., Bowen, J.E., *et al.* (2020). Mapping Neutralizing and
710 Immunodominant Sites on the SARS-CoV-2 Spike Receptor-Binding Domain by Structure-
711 Guided High-Resolution Serology. *Cell* 183, 1024-1042 e1021.
712 Pickering, S., Betancor, G., Galao, R.P., Merrick, B., Signell, A.W., Wilson, H.D., Kia Ik, M.T.,
713 Seow, J., Graham, C., Acors, S., *et al.* (2020). Comparative assessment of multiple COVID-
714 19 serological technologies supports continued evaluation of point-of-care lateral flow assays
715 in hospital and community healthcare settings. *PLoS Pathog* 16, e1008817.
716 Polack, F.P., Thomas, S.J., Kitchin, N., Absalon, J., Gurtman, A., Lockhart, S., Perez, J.L.,
717 Perez Marc, G., Moreira, E.D., Zerbini, C., *et al.* (2020). Safety and Efficacy of the BNT162b2
718 mRNA Covid-19 Vaccine. *N Engl J Med* 383, 2603-2615.
719 Ramasamy, M.N., Minassian, A.M., Ewer, K.J., Flaxman, A.L., Folegatti, P.M., Owens, D.R.,
720 Voysey, M., Aley, P.K., Angus, B., Babbage, G., *et al.* (2021). Safety and immunogenicity of
721 ChAdOx1 nCoV-19 vaccine administered in a prime-boost regimen in young and old adults
722 (COV002): a single-blind, randomised, controlled, phase 2/3 trial. *Lancet* 396, 1979-1993.
723 Raybould, M.I.J., Kovaltsuk, A., Marks, C., and Deane, C.M. (2021). CoV-AbDab: the
724 coronavirus antibody database. *Bioinformatics* 37, 734-735.
725 Rees-Spear, C., Muir, L., Griffith, S.A., Heaney, J., Aldon, Y., Snitselaar, J.L., Thomas, P.,
726 Graham, C., Seow, J., Lee, N., *et al.* (2021). The effect of spike mutations on SARS-CoV-2
727 neutralization. *Cell Rep*, 108890.
728 Robbiani, D.F., Gaebler, C., Muecksch, F., Lorenzi, J.C.C., Wang, Z., Cho, A., Agudelo, M.,
729 Barnes, C.O., Gazumyan, A., Finkin, S., *et al.* (2020). Convergent antibody responses to
730 SARS-CoV-2 in convalescent individuals. *Nature* 584, 437-442.
731 Rogers, T.F., Zhao, F., Huang, D., Beutler, N., Burns, A., He, W.T., Limbo, O., Smith, C.,
732 Song, G., Woehl, J., *et al.* (2020). Isolation of potent SARS-CoV-2 neutralizing antibodies and
733 protection from disease in a small animal model. *Science* 369, 956-963.
734 Rosa, A., Pye, V.E., Graham, C., Muir, L., Seow, J., Ng, K.W., Cook, N.J., Rees-Spear, C.,
735 Parker, E., Kassiotis, G., *et al.* (2021a). SARS-CoV-2 recruits a haem metabolite to evade
736 antibody immunity. *medRxiv*.
737 Rosa, A., Pye, V.E., Graham, C., Muir, L., Seow, J., Ng, K.W., Cook, N.J., Rees-Spear, C.,
738 Parker, E., Silva Dos Santos, M., *et al.* (2021b). SARS-CoV-2 can recruit a haem metabolite
739 to evade antibody immunity. *Sci Adv*.
740 Scheid, J.F., Mouquet, H., Feldhahn, N., Seaman, M.S., Velinzon, K., Pietzsch, J., Ott, R.G.,
741 Anthony, R.M., Zebroski, H., Hurley, A., *et al.* (2009). Broad diversity of neutralizing antibodies
742 isolated from memory B cells in HIV-infected individuals. *Nature* 458, 636-640.
743 Seow, J., Graham, C., Merrick, B., Acors, S., Pickering, S., Steel, K.J.A., Hemmings, O.,
744 O'Byrne, A., Kouphou, N., Galao, R.P., *et al.* (2020). Longitudinal observation and decline of
745 neutralizing antibody responses in the three months following SARS-CoV-2 infection in
746 humans. *Nat Microbiol* 5, 1598-1607.
747 Seydoux, E., Homad, L.J., MacCamy, A.J., Parks, K.R., Hurlburt, N.K., Jennewein, M.F.,
748 Akins, N.R., Stuart, A.B., Wan, Y.H., Feng, J., *et al.* (2020). Analysis of a SARS-CoV-2-
749 Infected Individual Reveals Development of Potent Neutralizing Antibodies with Limited
750 Somatic Mutation. *Immunity* 53, 98-105 e105.
751 Siu, J.H.Y. (2021). Two subsets of human marginal zone B cells resolved by global analysis
752 of lymphoid tissues and blood. *bioRxiv*.
753 Supasa, P., Zhou, D., Dejnirattisai, W., Liu, C., Mentzer, A.J., Ginn, H.M., Zhao, Y.,
754 Duyvesteyn, H.M.E., Nutalai, R., Tuekprakhon, A., *et al.* (2021). Reduced neutralization of
755 SARS-CoV-2 B.1.1.7 variant by convalescent and vaccine sera. *Cell* 184, 2201-2211 e2207.

756 Suryadevara, N., Shrihari, S., Gilchuk, P., VanBlargan, L.A., Binshtein, E., Zost, S.J., Nargi,
757 R.S., Sutton, R.E., Winkler, E.S., Chen, E.C., *et al.* (2021). Neutralizing and protective human
758 monoclonal antibodies recognizing the N-terminal domain of the SARS-CoV-2 spike protein.
759 *Cell* 184, 2316-2331 e2315.

760 Thompson, C.P., Grayson, N.E., Paton, R.S., Bolton, J.S., Lourenco, J., Penman, B.S., Lee,
761 L.N., Odon, V., Mongkolsapaya, J., Chinnakannan, S., *et al.* (2020). Detection of neutralising
762 antibodies to SARS-CoV-2 to determine population exposure in Scottish blood donors
763 between March and May 2020. *Euro Surveill* 25.

764 Tiller, T., Meffre, E., Yurasov, S., Tsuiji, M., Nussenzweig, M.C., and Wardemann, H. (2008).
765 Efficient generation of monoclonal antibodies from single human B cells by single cell RT-PCR
766 and expression vector cloning. *J Immunol Methods* 329, 112-124.

767 Tortorici, M.A., Beltramello, M., Lempp, F.A., Pinto, D., Dang, H.V., Rosen, L.E., McCallum,
768 M., Bowen, J., Minola, A., Jaconi, S., *et al.* (2020). Ultrapotent human antibodies protect
769 against SARS-CoV-2 challenge via multiple mechanisms. *Science* 370, 950-957.

770 von Boehmer, L., Liu, C., Ackerman, S., Gitlin, A.D., Wang, Q., Gazumyan, A., and
771 Nussenzweig, M.C. (2016). Sequencing and cloning of antigen-specific antibodies from
772 mouse memory B cells. *Nat Protoc* 11, 1908-1923.

773 Voysey, M., Clemens, S.A.C., Madhi, S.A., Weckx, L.Y., Folegatti, P.M., Aley, P.K., Angus,
774 B., Baillie, V.L., Barnabas, S.L., Bhorat, Q.E., *et al.* (2021). Safety and efficacy of the ChAdOx1
775 nCoV-19 vaccine (AZD1222) against SARS-CoV-2: an interim analysis of four randomised
776 controlled trials in Brazil, South Africa, and the UK. *Lancet* 397, 99-111.

777 Wall, E.C., Wu, M., Harvey, R., Kelly, G., Warchal, S., Sawyer, C., Daniels, R., Adams, L.,
778 Hobson, P., Hatipoglu, E., *et al.* (2021). AZD1222-induced neutralising antibody activity
779 against SARS-CoV-2 Delta VOC. *Lancet* 398, 207-209.

780 Walsh, E.E., Frenck, R.W., Jr., Falsey, A.R., Kitchin, N., Absalon, J., Gurtman, A., Lockhart,
781 S., Neuzil, K., Mulligan, M.J., Bailey, R., *et al.* (2020). Safety and Immunogenicity of Two RNA-
782 Based Covid-19 Vaccine Candidates. *N Engl J Med* 383, 2439-2450.

783 Wang, L., Zhou, T., Zhang, Y., Yang, E.S., Schramm, C.A., Shi, W., Pegu, A., Oloniniyi, O.K.,
784 Henry, A.R., Darko, S., *et al.* (2021a). Ultrapotent antibodies against diverse and highly
785 transmissible SARS-CoV-2 variants. *Science* 373.

786 Wang, P., Casner, R.G., Nair, M.S., Wang, M., Yu, J., Cerutti, G., Liu, L., Kwong, P.D., Huang,
787 Y., Shapiro, L., *et al.* (2021b). Increased resistance of SARS-CoV-2 variant P.1 to antibody
788 neutralization. *Cell Host Microbe* 29, 747-751 e744.

789 Wang, P., Nair, M.S., Liu, L., Iketani, S., Luo, Y., Guo, Y., Wang, M., Yu, J., Zhang, B., Kwong,
790 P.D., *et al.* (2021c). Antibody Resistance of SARS-CoV-2 Variants B.1.351 and B.1.1.7.
791 *Nature*.

792 Wang, Z., Schmidt, F., Weisblum, Y., Muecksch, F., Barnes, C.O., Finkin, S., Schaefer-
793 Babajew, D., Cipolla, M., Gaebler, C., Lieberman, J.A., *et al.* (2021d). mRNA vaccine-elicited
794 antibodies to SARS-CoV-2 and circulating variants. *Nature* 592, 616-622.

795 Wibmer, C.K., Ayres, F., Hermanus, T., Madzivhandila, M., Kgagudi, P., Oosthuysen, B.,
796 Lambson, B.E., de Oliveira, T., Vermeulen, M., van der Berg, K., *et al.* (2021). SARS-CoV-2
797 501Y.V2 escapes neutralization by South African COVID-19 donor plasma. *Nat Med*.

798 Yuan, M., Liu, H., Wu, N.C., Lee, C.D., Zhu, X., Zhao, F., Huang, D., Yu, W., Hua, Y., Tien,
799 H., *et al.* (2020a). Structural basis of a shared antibody response to SARS-CoV-2. *Science*
800 369, 1119-1123.

801 Yuan, M., Liu, H., Wu, N.C., and Wilson, I.A. (2020b). Recognition of the SARS-CoV-2
802 receptor binding domain by neutralizing antibodies. *Biochem Biophys Res Commun*.

803 Yuan, M., Wu, N.C., Zhu, X., Lee, C.D., So, R.T.Y., Lv, H., Mok, C.K.P., and Wilson, I.A.
804 (2020c). A highly conserved cryptic epitope in the receptor binding domains of SARS-CoV-2
805 and SARS-CoV. *Science* 368, 630-633.

806 Zhou, D., and al, e. (2021). Evidence of escape of SARS-CoV-2 variant B.1.351 from natural
807 and vaccine induced sera. *Cell*.

808 Zhou, D., Dejnirattisai, W., Supasa, P., Liu, C., Mentzer, A.J., Ginn, H.M., Zhao, Y.,
809 Duyvesteyn, H.M.E., Tuekprakhon, A., Nutalai, R., *et al.* (2021). Evidence of escape of SARS-
810 CoV-2 variant B.1.351 from natural and vaccine-induced sera. *Cell*.

811 Zufferey, R., Nagy, D., Mandel, R.J., Naldini, L., and Trono, D. (1997). Multiply attenuated
812 lentiviral vector achieves efficient gene delivery in vivo. *Nat Biotechnol* *15*, 871-875.
813